ISSN: 2639-7536

Research Article

Petroleum and Chemical Industry International

Seismic Shear Wave Velocity Fractal Dimension for Characterizing Shajara Reservoirs of the Permo-Carboniferous Shajara Formation, Saudi Arabia

Khalid Elyas Mohamed Elameen Alkhidir

King Saud University, Saudi Arabia

*Corresponding author
Khalid Elyas Mohamed Elameen Alkhidir, Ph.D. Department of Petroleum and Natural Gas Engineering, College of Engineering, King Saud University, Saudi Arabia, E-mail: kalkhidir@ksu.edu.sa

Submitted: 18 June 2019; **Accepted**: 25 June 2019; **Published**: 22 July 2019

Abstract

The quality and assessment of a reservoir can be documented in details by the application of seismic shear wave. This research aims to calculate fractal dimension from the relationship among seismic shear wave velocity, maximum seismic shear wave velocity and wetting phase saturation and to approve it by the fractal dimension derived from the relationship among capillary pressure and wetting phase saturation. Two equations for calculating the fractal dimensions have been employed. The first one describes the functional relationship between wetting phase saturation, seismic shear wave velocity and maximum seismic shear wave velocity and fractal dimension. The second equation implies to the wetting phase saturation as a function of capillary pressure and the fractal dimension. Two procedures for obtaining the fractal dimension have been utilized. The first procedure was done by plotting the logarithm of the ratio between seismic shear wave velocity and maximum seismic shear wave velocity versus logarithm wetting phase saturation. The slope of the first procedure = 3- Df (fractal dimension). The second procedure for obtaining the fractal dimension was determined by plotting the logarithm of capillary pressure versus the logarithm of wetting phase saturation. The slope of the second procedure = Df -3. On the basis of the obtained results of the fabricated stratigraphic column and the attained values of the fractal dimension, the sandstones of the Shajara reservoirs of the Shajara Formation were divided here into three units.

Keywords: Shajara Reservoirs, Shajara Formation, seismic shear wave velocity fractal dimension, Capillary pressure fractal dimension

Introduction

Seismo electric effects related to electro kinetic potential, dielectric permitivity, pressure gradient, fluid viscosity, and electric conductivty was first reported by Frenkel J [1]. Capillary pressure follows the scaling law at low wetting phase saturation was reported by Li K and Williams W [2]. Seismo electric phenomenon by considering electro kinetic coupling coefficient as a function of effective charge density, permeability, fluid viscosity and electric conductivity was reported by Revil A and Jardani A [3]. The magnitude of seismo electric current depends on porosity, pore size, zeta potential of the pore surfaces, and elastic properties of the matrix was investigated by Dukhin A [4]. The tangent of the ratio of converted electic field to pressure is approximately in inverse proportion to permeability was studied by Guan W [5]. Permeability inversion from seismoelectric log at low frequency was studied by Hu H [6]. They reported that, the tangent of the ratio among electric excitation intensity and pressure field is a function of porosity, fluid viscosity, frequency, tortuosity and fluid density and Dracy permeability. A decrease of seismo electric frequencies with increasing water content was reported by Borde C [7]. An increase of seismo electric transfer function with increasing water saturation was studied byJardani A and Revil A [8]. An increase of dynamic seismo electric transfer function with decreasing fluid conductivity was described by Holzhauer J [9]. The amplitude of seismo electric signal increases with increasing permeability which means that the seismo electric effects are directly related to the permeability and can be used to study the permeability of the reservoir was illustrated by Ping R [10]. Seismo electric coupling is frequency dependent and decreases expontialy when frequency increases was demonstrated by Djuraev U [11]. An increase of permeability with increasing pressure head and bubble pressure fractal dimension was reported by Alkhidir KEME [12, 13]. An increase of geometric relaxationtime of induced polarization fractal dimension with permeability increasing and grain size was described by Alkhidir KEME [14,15].

Materials and Methods

Sandstone samples were collected from the surface type section of the Permo-Carboniferous Shajara Formation, latitude 26° 52' 17.4", longitude 43° 36' 18". (Figure1).

Porosity was measured on collected samples using mercury intrusion Porosimetry and permeability was derived from capillary pressure data. The purpose of this paper is to obtain seismic shear wave velocity fractal dimension and to confirm it by capillary pressure fractal dimension. The fractal dimension of the first procedure is

determined from the positive slope of the plot of logarithm of the ratio of seismic shear wave velocity to maximum seismic shear wave velocity log (SSWV1/4/SSWV1/4max) versus log wetting phase saturation (logSw). Whereas the fractal dimension of the second procedure is determined from the negative slope of the plot of logarithm of log capillary pressure (log Pc) versus logarithm of wetting phase saturation (log Sw).

The seismic shear wave velocity can be scaled as

$$\mathbf{Sw} = \left[\frac{\mathbf{SSWV}^{\frac{1}{4}}}{\mathbf{SSWV}^{\frac{1}{4}}_{\mathbf{max}}}\right]^{[3-\mathbf{Df}]} \quad 1$$

Where Sw the water saturation, SSWV the seismic shear wave velocity in meter / second, $SSWV_{max}$ the maximum shear wave velocity in meter / second and Df the fractal dimension.

Equation 1 can be proofed from

$$\mathbf{H} = \left[\frac{\Phi * \varepsilon 0 * \mathbf{Kf} * \zeta * \rho f * \sqrt{\frac{G}{\rho} * \frac{du}{dt}}}{\alpha\infty * \eta}\right] \quad 2$$

Where H the seismo magnetic field generated from shear wave velocity in ampere / meter, Φ the porosity, ε0 permittivity of free scape in Faraday / meter, kf dielectric constant of the fluid, ζ the zeta potential in volt, ρf the fluid density in kilo gram /meter, G the shear modulus in pascal, ρ bulk density in kilo gram /m3, dU/dt the radial grain velocity in meter / second, α∞ the tortuosity, and nd η the fluid viscosity in pascal * second.

The density ρf can be scaled as

$$\rho f = \left[\frac{\mathbf{m}}{\mathbf{V}}\right] \quad 3$$

Where ρf the fluid density in kilo gram /meter, m the mass in kilo gram, and V the velocity in cubic meter.

Insert equation 3 into equation 2

$$\mathbf{H} = \left[\frac{\Phi * \varepsilon 0 * \mathbf{Kf} * \zeta * \mathbf{m} * \sqrt{\frac{G}{\rho} * \frac{du}{dt}}}{\alpha\infty * \eta * \mathbf{V}}\right] \quad 4$$

The mass m can be scaled as

$$\mathbf{m} = \left[\frac{\mathbf{F}}{\mathbf{g}}\right] \quad 5$$

Where m the mass in kilo gram, F the force in newton, g the acceleration in meter / square second

Insert equation 5 into equation 4

$$\mathbf{H} = \left[\frac{\Phi * \varepsilon 0 * \mathbf{Kf} * \zeta * \mathbf{F} * \sqrt{\frac{G}{\rho} * \frac{du}{dt}}}{\alpha\infty * \eta * \mathbf{V} * \mathbf{g}}\right] \quad 6$$

The acceleration g can be scaled as

$$\mathbf{g} = \left[\frac{\mathbf{E}}{\psi}\right] \quad 7$$

Where g the acceleration in meter / square second, E the electric field in volt / meter, ψ the seismo electric transfer function in volt * square second / square meter

Insert equation 7 into equation 6

$$\mathbf{H} = \left[\frac{\Phi * \varepsilon 0 * \mathbf{Kf} * \zeta * \mathbf{F} * \psi \sqrt{\frac{G}{\rho} * \frac{du}{dt}}}{\alpha\infty * \eta * \mathbf{V} * \mathbf{E}}\right] \quad 8$$

The electric field E field can be scaled as

$$\mathbf{E} = \left[\frac{\mathbf{vol}}{\mathbf{CEK}}\right] \quad 9$$

Where E the electric field in volt / meter, vol the velocity in meter / second, CEK the electro kinetic coefficient in ampere / pascal * meter

Insert equation 9 into equation 8

$$\mathbf{H} = \left[\frac{\Phi * \varepsilon 0 * \mathbf{Kf} * \zeta * \mathbf{F} * \psi * \mathbf{CEK} \sqrt{\frac{G}{\rho} * \frac{du}{dt}}}{\alpha\infty * \eta * \mathbf{V} * \mathbf{vol}}\right] \quad 10$$

The velocity vol can be scaled as

$$\mathbf{vol} = \left[\frac{\mathbf{Q}}{\mathbf{A}}\right] \quad 11$$

$$\mathbf{H} = \left[\frac{\Phi * \varepsilon 0 * \mathbf{Kf} * \zeta * \mathbf{F} * \psi * \mathbf{CEK} * \mathbf{A} \sqrt{\frac{G}{\rho} * \frac{du}{dt}}}{\alpha\infty * \eta * \mathbf{V} * \mathbf{Q}}\right] \quad 12$$

The flow rate Q can be scaled as

$$\mathbf{Q} = \left[\frac{3.14 * \mathbf{r}^4 * \Delta P}{8 * \eta * \mathbf{L}}\right] \quad 13$$

Where Q the flow rate in cubic meter / second, k the permeability in square meter, A the area in square meter, ΔP the differential pressure in pascal, η the fluid viscosity in pascal * second, L the capillary length in meter

Insert equation 13 into equation 12

$$\mathbf{H} = \left[\frac{\Phi * \varepsilon 0 * \mathbf{Kf} * \zeta * \mathbf{F} * \psi * \mathbf{CEK} * \mathbf{A} * 8 * \eta * \mathbf{L} \sqrt{\frac{G}{\rho} * \frac{du}{dt}}}{\alpha\infty * \eta * \mathbf{V} * 3.14 * \mathbf{r}^4 * \Delta P}\right] \quad 14$$

The seismic shear wave velocity can be scaled as

$$\mathbf{SSWV} = \sqrt{\left[\frac{\mathbf{G}}{\rho}\right]} \quad 15$$

Where SSWV seismic shear wave velocity in meter / second, G the shear modules in pascal, and ρ the bulk density in kilo gram / cubic meter

Insert equation 15 into equation 14

$$\mathbf{H} = \left[\frac{\Phi * \varepsilon 0 * \mathbf{Kf} * \zeta * \mathbf{F} * \psi * \mathbf{CEK} * \mathbf{A} * 8 * \eta * \mathbf{L} * \mathbf{SSWV} \sqrt{\frac{du}{dt}}}{\alpha\infty * \eta * \mathbf{V} * 3.14 * \mathbf{r}^4 * \Delta P}\right] \quad 16$$

Equation 16 after rearrange of pore radius will become

$$\mathbf{r}^4 = \left[\frac{\Phi * \varepsilon 0 * \mathbf{Kf} * \zeta * \mathbf{F} * \psi * \mathbf{CEK} * \mathbf{A} * 8 * \eta * \mathbf{L} * \mathbf{SSWV} \sqrt{\frac{du}{dt}}}{\alpha\infty * \eta * \mathbf{V} * 3.14 * \mathbf{H} * \Delta P}\right] \quad 17$$

The maximum pore radius can be scaled as

$$r^4_{max} = \left[\frac{\Phi * \varepsilon 0 * Kf * \zeta * F * \psi * CEK * A * 8 * \eta * L * SSWV_{max}\sqrt{\frac{du}{dt}}}{\alpha\infty * \eta * V * 3.14 * H * \Delta P}\right] \quad 18$$

Divide equation 17 by equation 18

$$\left[\frac{r^4}{r^4_{max}}\right] = \left[\frac{\left[\frac{\Phi*\varepsilon0*Kf*\zeta*F*\psi*CEK*A*8*\eta*L*SSWV\sqrt{\frac{du}{dt}}}{\alpha\infty*\eta*V*3.14*H*\Delta P}\right]}{\left[\frac{\Phi*\varepsilon0*Kf*\zeta*F*\psi*CEK*A*8*\eta*L*SSWV_{max}\sqrt{\frac{du}{dt}}}{\alpha\infty*\eta*V*3.14*H*\Delta P}\right]}\right] \quad 19$$

Equation 19 after simplification will become

$$\left[\frac{r^4}{r^4_{max}}\right] = \left[\frac{SSWV}{SSWV_{max}}\right] \quad 20$$

Take the fourth root of equation 20

$$\sqrt[4]{\left[\frac{r^4}{r^4_{max}}\right]} = \sqrt[4]{\left[\frac{SSWV}{SSWV_{max}}\right]} \quad 21$$

Equation 21 after simplification will become

$$\left[\frac{r}{r_{max}}\right] = \left[\frac{SSWV^{\frac{1}{4}}}{SSWV^{\frac{1}{4}}_{max}}\right] \quad 22$$

Take the logarithm of equation 22

$$\log\left[\frac{r}{r_{max}}\right] = \log\left[\frac{SSWV^{\frac{1}{4}}}{SSWV^{\frac{1}{4}}_{max}}\right] \quad 23$$

$$\text{But; } \log\left[\frac{r}{r_{max}}\right] = \left[\frac{\log Sw}{3 - Df}\right] \quad 24$$

Insert equation 24 into equation 23

$$\left[\frac{\log Sw}{3 - Df}\right] = \log\left[\frac{SSWV^{\frac{1}{4}}}{SSWV^{\frac{1}{4}}_{max}}\right] \quad 25$$

Equation 25 after log removal will become

$$Sw = \left[\frac{SSWV^{\frac{1}{4}}}{SSWV^{\frac{1}{4}}_{max}}\right]^{[3-Df]} \quad 26$$

Equation 26 the proof of equation 1 which relates the water saturation, seismic shear wave velocity, maximum shear wave velocity and the fractal dimension.

The capillary pressure can be scaled as

$$Sw = [Df - 3] * Pc * constant \quad 27$$

Where Sw the water saturation, Pc the capillary pressure and Df the fractal dimension.

Results and Discussion

Based on field observation the Shajara Reservoirs of the Permo-Carboniferous Shajara Formation were divided here into three units as described in Figure1.These units from bottom to top are: Lower Shajara Reservoir, Middle Shajara reservoir, and Upper Shajara Reservoir. Their attained results of the Seismic shear wave velocityfractal dimension and capillary pressure fractal dimension are shown in Table 1. Based on the achieved results it was found that the Seismic shear wave velocityfractal dimension is equal to the capillary pressure fractal dimension. The maximum value of the fractal dimension was found to be 2.7872 allocated to sample SJ13 from the Upper Shajara Reservoir as verified in Table 1. Whereas the minimum value of the fractal dimension 2.4379 was reported from sample SJ3 from the Lower Shajara reservoir as shown in Table1. The Seismic shear wave velocity fractal dimension and capillary pressure fractal dimension were detected to increase with increasing permeability as proofed in Table1 owing to the possibility of having interconnected channels.

Table 1: Petrophysical model showing the three Shajara Reservoir Units with their corresponding values of Seismic shear wave velocityfractal dimension and capillary pressure fractal dimension

Formation	Reservoir	Sample	Porosity %	k (md)	Positive slope of the first procedure Slope=3-Df	Negative slope of the second procedure Slope=Df-3	Seismic shear wave velocityfractal dimension	Capillary pressure fractal dimension
Permo-Carboniferous Shajara Formation	Upper	SJ13	25	973	0.2128	-0.2128	2.7872	2.7872
	Shajara	SJ12	28	1440	0.2141	-0.2141	2.7859	2.7859
	Reservoir	SJ11	36	1197	0.2414	-0.2414	2.7586	2.7586
	Middle	SJ9	31	1394	0.2214	-0.2214	2.7786	2.7786
	Shajara	SJ8	32	1344	0.2248	-0.2248	2.7752	2.7752
	Reservoir	SJ7	35	1472	0.2317	-0.2317	2.7683	2.7683
	Lower	SJ4	30	176	0.3157	-0.3157	2.6843	2.6843
	Shajara	SJ3	34	56	0.5621	-0.5621	2.4379	2.4379
	Reservoir	SJ2	35	1955	0.2252	-0.2252	2.7748	2.7748
		SJ1	29	1680	0.2141	-0.2141	2.7859	2.7859

The Lower Shajara reservoir was symbolized by six sandstone samples (Figure 1), four of which label as SJ1, SJ2, SJ3 and SJ4 were carefully chosen for capillary pressure measurement as proven in Table1. Their positive slopes of the first procedure log of the Seismic shear wave velocityto maximum Seismic shear wave velocityversus log wetting phase saturation (Sw) and negative slopes of the second procedure log capillary pressure (Pc) versus log wetting phase saturation (Sw) are clarified in Figure 2, Figure 3, Figure 4, Figure 5 and Table 1. Their Seismic shear wave velocityfractal dimension and capillary pressure fractal dimension values are revealed in Table 1. As we proceed from sample SJ2 to SJ3 a pronounced reduction in permeability due to compaction was described from 1955 md to 56 md which reflects decrease in Seismic shear wave velocityfractal dimension from 2.7748 to 2.4379 as quantified in table 1. Again, an increase in grain size and permeability was proved from sample SJ4 whose Seismic shear wave velocityfractal dimension and capillary pressure fractal dimension was found to be 2.6843 as described in Table 1.

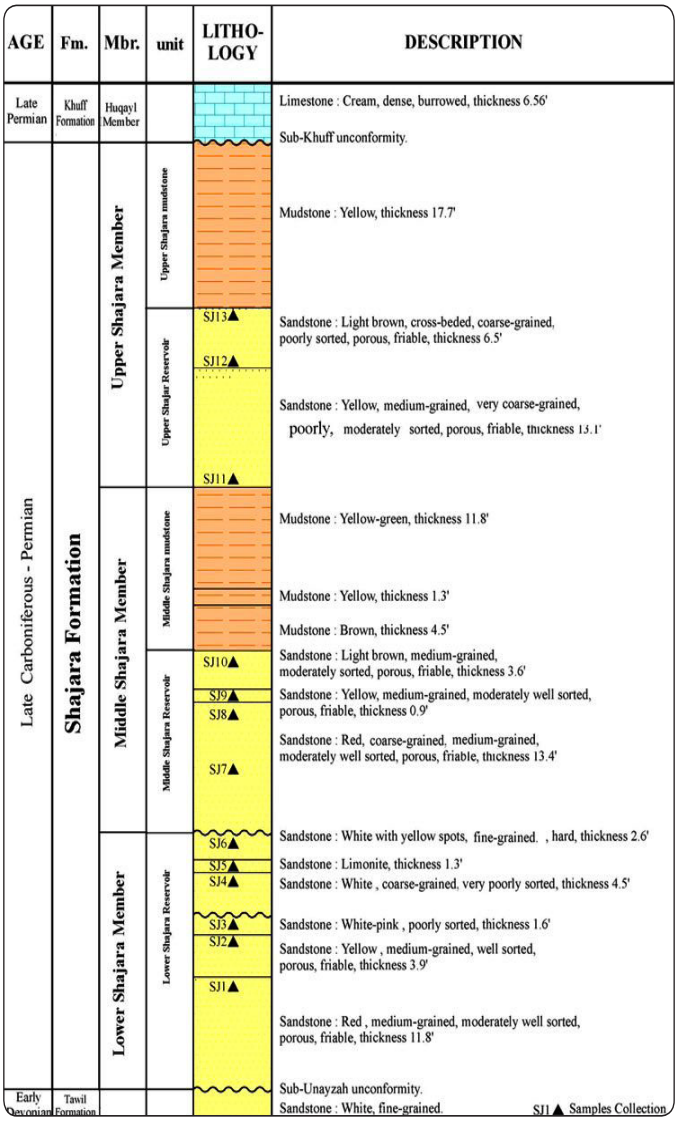

Figure 1: Surface type section of the Shajara Reservoirs of the Permo-Carboniferous Shajara Formation at latitude 26° 52' 17.4" longitude 43° 36' 18"

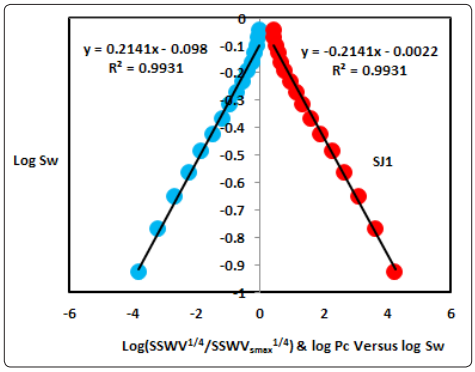

Figure 2: Log ($SSWV^{1/4}/SSWV^{1/4}_{max}$)& log pc versus log Sw for sample SJ1

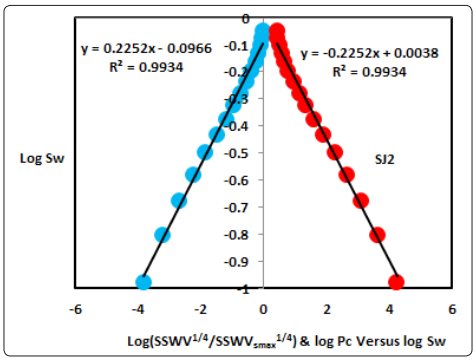

Figure 3: Log ($SSWV^{1/4}/SSWV^{1/4}_{max}$) & log pc versus log Sw for sample SJ2

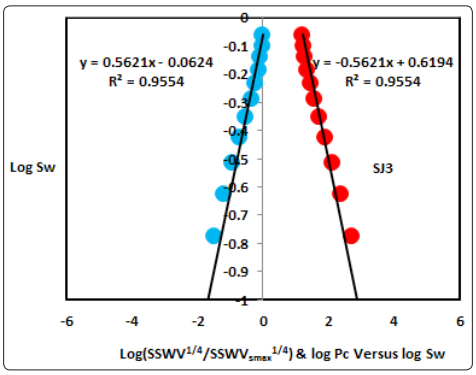

Figure 4: Log ($SSWV^{1/4}/SSWV^{1/4}_{max}$) & log pc versus log Sw for sample SJ3

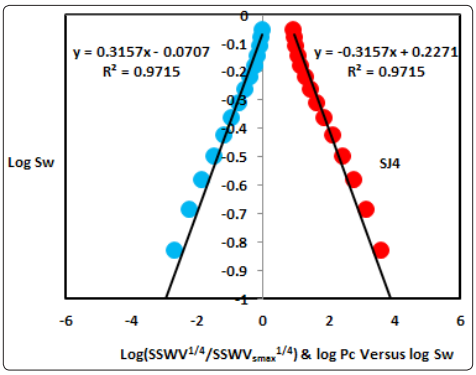

Figure 5: Log ($SSWV^{1/4}/SSWV^{1/4}_{max}$) & log pc versus log Sw for sample SJ4

In contrast, the Middle Shajara reservoir which is separated from the Lower Shajara reservoir by an unconformity surface as revealed in Figure 1. It was nominated by four samples (Figure 1), three of which named as SJ7, SJ8, and SJ9 as illuminated in Table1 were chosen for capillary measurements as described in Table 1. Their positive slopes of the first procedure and negative slopes of the second procedure are shown in Figure 6, Figure 7 and Figure 8 and Table 1. Furthermore, their Seismic shear wave velocityfractal dimensions and capillary pressure fractal dimensions show similarities as defined in Table 1.Their fractal dimensions are higher than those of samples SJ3 and SJ4 from the Lower Shajara Reservoir due to an increase in their permeability as explained in table 1.

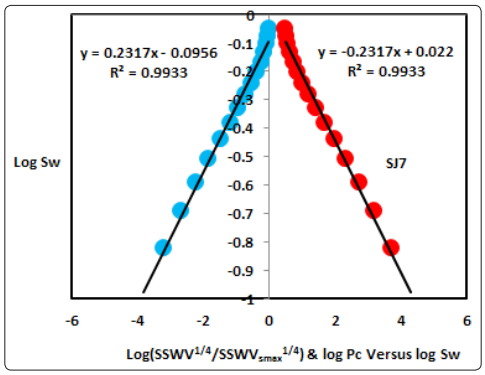

Figure 6: Log ($SSWV^{1/4}/SSWV^{1/4}_{max}$) & log pc versus log Sw for sample SJ7

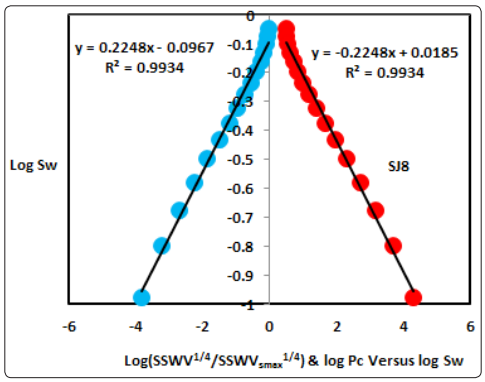

Figure 7: Log ($SSWV^{1/4}/SSWV^{1/4}_{max}$) & log pc versus log Sw for sample SJ8

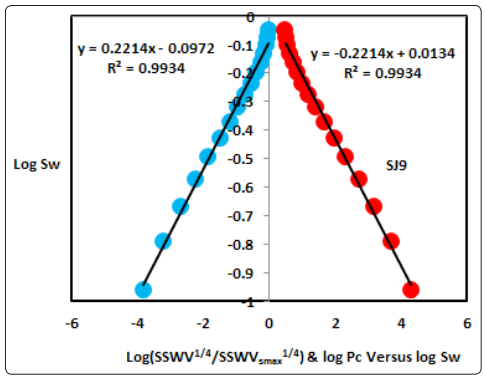

Figure 8: Log ($SSWV^{1/4}/SSWV^{1/4}_{max}$) & log pc versus log Sw for sample SJ9

On the other hand, the Upper Shajara reservoir was separated from the Middle Shajara reservoir by yellow green mudstone as shown in Figure 1. It is defined by three samples so called SJ11, SJ12, SJ13 as explained in Table 1. Their positive slopes of the first procedure and negative slopes of the second procedure are displayed in Figure 9, Figure 10 and Figure 11 and Table 1. Moreover, their Seismic shear wave velocityfractal dimension and capillary pressure fractal dimension are also higher than those of sample SJ3 and SJ4 from the Lower Shajara Reservoir due to an increase in their permeability as simplified in table 1.

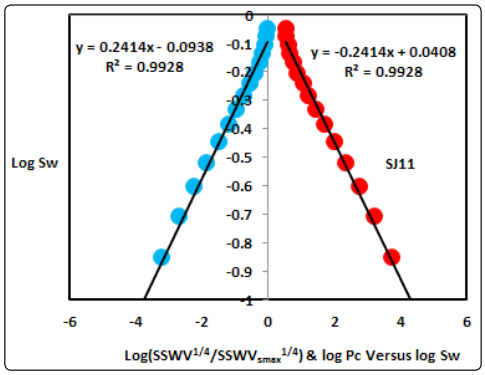

Figure 9: Log ($SSWV^{1/4}/SSWV^{1/4}_{max}$) & log pc versus log Sw for sample SJ11

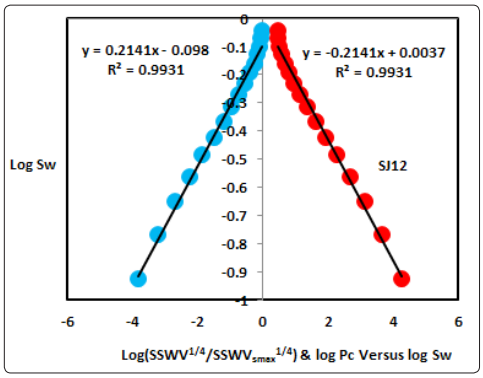

Figure 10: Log ($SSWV^{1/4}/SSWV^{1/4}_{max}$) & log pc versus log Sw for sample SJ12

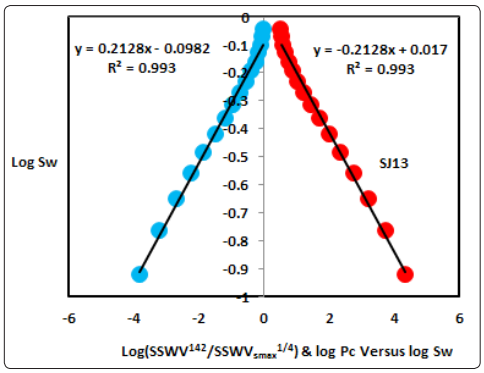

Figure 11: Log ($SSWV^{1/4}/SSWV^{1/4}_{max}$) & log pc versus log Sw for sample SJ13

Overall a plot of positive slope of the first procedure versus negative slope of the second procedure as described in Figure 12 reveals three permeable zones of varying Petrophysical properties. These reservoir zones were also confirmed by plotting Seismic shear wave velocityfractal dimension versus capillary pressure fractal dimension as described in Figure 13. Such variation in fractal dimension can account for heterogeneity which is a key parameter in reservoir quality assessment.

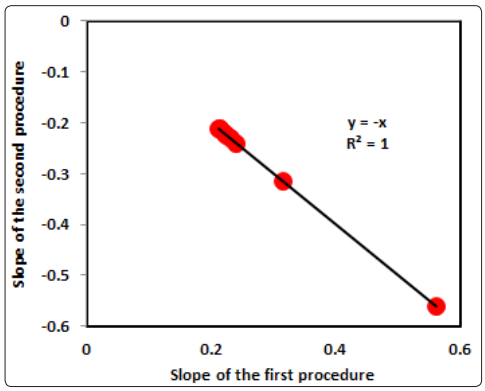

Figure 12: Slope of the first procedure versus slope of the second procedure

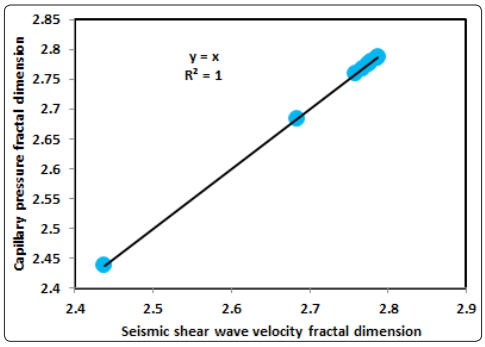

Figure 13: Seismic shear wave velocityvelocity fractal dimension versus capillary pressure fractal dimension

Conclusion

- The sandstones of the Shajara Reservoirs of the permo-Carboniferous Shajara Formation were divided here into three units based on Seismic shear wave velocity fractal dimension.
- The Units from base to top are: Lower Shajara Seismic Shear Wave VelocityFractal dimension Unit, Middle Shajara Seismic Shear Wave VelocityFractal Dimension Unit, and Upper Shajara Seismic Shear Wave VelocityFractal Dimension Unit.
- These units were also proved by capillary pressure fractal dimension.
- The fractal dimension was found to increase with increasing grain size and permeability owing to possibility of having interconnected channels.

Acknowledgement

The author would to thank King Saud University, College of Engineering, Department of Petroleum and Natural Gas Engineering, Department of Chemical Engineering, Research Centre at College of Engineering, College of Science, Department of Geology, and King Abdullah Institute for research and Consulting Studies for their supports.

References

1. Frenkel J (1944) On the theory of seismic and seismoelectric phenomena in a moist soil. Journal of physics 3: 230-241.
2. Li K, Williams W (2007) Determination of capillary pressure function from resistivity data. Transport in Porous Media 67: 1-15.
3. Revil A, Jardani A (2010) Seismo electric response of heavy oil reservoirs: theory and numerical modelling. Geophysical J International 180: 781-797.
4. Dukhin A, Goetz P, Thommes M (2010) Seismoelectric effect: a non-isochoric streaming current.1 Experiment. J Colloid Interface Sci 345: 547-553.
5. Guan W, Hu H, Wang Z (2012) Permeability inversion from low-frequency seismoelectric logs in fluid- saturated porous formations. Geophys Prospect 61: 120-133.
6. Hu H, Guan W, Zhao W (2012) Theoretical studies of permeability inversion from seismoelectric logs. Geophysical Research Abstracts 14: EGU2012-6725-1 2012 EGU General Assembly.
7. Borde C, S en echal P Barri`ere J, Brito D, Normandin E et al., (2015) Impact of water saturation on seismoelectric transfer functions: a laboratory study of co-seismic phenomenon. Geophysical J International 200: 1317-1335.
8. Jardani A, Revil A (2015) Seismoelectric couplings in a poroelastic material containing two immiscible fluid phases. Geophysical Journal International 202: 850-870.
9. Holzhauer J, Brito D, Bordes C, Brun Y, Guatarbes B (2016) Experimental quantification of the seismoelectric transfer function and its dependence on conductivity and saturation in loose sand. Geophys Prospect 65: 1097-1120.
10. Rong Peng, Jian-Xing Wei, Bang-Rang Di, Pin-Bo Ding, Zi-Chun Liu (2016) Experimental research on seismoelectric effects in sandstone. Applied Geophysics 13: 425-436.
11. Djuraev U, Jufar S R, Vasant P (2017) Numerical Study of frequency-dependent seismo electric coupling in partially-saturated porous media. MATEC Web of Conferences 87, 02001.
12. Alkhidir KEME (2017) Pressure head fractal dimension for characterizing Shajara Reservoirs of the Shajara Formation of the Permo-Carboniferous Unayzah Group, Saudi Arabia. Arch Pet Environ Bio techno l2: 1-7.
13. Al-Khidir KE (2018) On Similarity of Pressure Head and Bubble Pressure Fractal Dimensions for Characterizing Permo-Carboniferous Shajara Formation, Saudi Arabia. J Indust Pollut Toxic 1: 1-10.
14. Alkhidir KEME (2018) Geometric relaxation time of induced polarization fractal dimension for characterizing Shajara Reservoirs of the Shajara Formation of the Permo-Carboniferous Unayzah Group, Saudi Arabia, Scifed J Petroleum 2: 1-6.
15. Alkhidir KEME (2018) Geometric relaxation time of induced polarization fractal dimension for characterizing Shajara Reservoirs of the Shajara formation of the Permo-Carboniferous Unayzah Group-Permo. Int J Pet and Res 2: 105-108.